Structural connectivity–based segmentation of the thalamus and prediction of tremor improvement following thalamic deep brain stimulation of the ventral intermediate nucleus

Erik H. Middlebrooks[a,b,*], Ibrahim S. Tuna[c], Leonardo Almeida[d,e], Sanjeet S. Grewal[b], Joshua Wong[d], Michael G. Heckman[f], Elizabeth R. Lesser[f], Markus Bredel[g], Kelly D. Foote[e,h], Michael S. Okun[d,e], Vanessa M. Holanda[h,i]

[a] Department of Radiology, Mayo Clinic, Jacksonville, FL, USA
[b] Department of Neurologic Surgery, Mayo Clinic, Jacksonville, FL, USA
[c] Department of Radiology, University of Florida, Gainesville, FL, USA
[d] Department of Neurology, University of Florida, Gainesville, FL, USA
[e] Fixel Center for Neurological Diseases, University of Florida, Gainesville, FL, USA
[f] Division of Biomedical Statistics and Informatics, Mayo Clinic, Jacksonville, FL, USA
[g] Department of Radiation Oncology, University of Alabama at Birmingham, Birmingham, AL, USA
[h] Department of Neurosurgery, University of Florida, Gainesville, FL, USA
[i] Center of Neurology and Neurosurgery Associates (NeuroCENNA), BP-A Beneficência Portuguesa de São Paulo, São Paulo, Brazil

ARTICLE INFO

ABSTRACT

Objectives: Traditional targeting methods for thalamic deep brain stimulation (DBS) performed to address tremor have predominantly relied on indirect atlas-based methods that focus on the ventral intermediate nucleus despite known variability in thalamic functional anatomy. Improvements in preoperative targeting may help maximize outcomes and reduce thalamic DBS–related complications. In this study, we evaluated the ability of thalamic parcellation with structural connectivity–based segmentation (SCBS) to predict tremor improvement following thalamic DBS.

Methods: In this retrospective analysis of 40 patients with essential tremor, hard segmentation of the thalamus was performed by using probabilistic tractography to assess structural connectivity to 7 cortical targets. The volume of tissue activated (VTA) was modeled in each patient on the basis of the DBS settings. The volume of overlap between the VTA and the 7 thalamic segments was determined and correlated with changes in preoperative and postoperative Fahn-Tolosa-Marin Tremor Rating Scale (TRS) scores by using multivariable linear regression models.

Results: A significant association was observed between greater VTA in the supplementary motor area (SMA) and premotor cortex (PMC) thalamic segment and greater improvement in TRS score when considering both the raw change ($P = .001$) and percentage change ($P = .011$). In contrast, no association was observed between change in TRS score and VTA in the primary motor cortex thalamic segment ($P \geq .19$).

Conclusions: Our data suggest that greater VTA in the thalamic SMA/PMC segment during thalamic DBS was associated with significant improvement in TRS score in patients with tremor. These findings support the potential role of thalamic SCBS as an independent predictor of tremor improvement in patients who receive thalamic DBS.

1. Introduction

Tremor is a common and often debilitating symptom associated with many neurological disorders such as Parkinson disease, dystonia, and essential tremor (ET). ET has been regarded as the most common pathologic tremor disorder (Louis and Ottman, 2014; Dogu et al., 2003). Although the underlying oscillators of many tremor syndromes remain unknown, the collective evidence regarding ET suggests that the cerebello-thalamo-cortical pathway is central to tremor network dysfunction (Coenen et al., 2014). Many invasive and noninvasive surgical treatment options target modulation of this network (Coenen et al., 2014; Louis, 2001; Benabid et al., 1996; Higuchi et al., 2015; Zhang et al., 2010).

One of the most widely targeted brain regions for tremor treatment is the ventral intermediate nucleus (VIM) of the thalamus (Foote and Okun, 2005; Mehanna et al., 2014). Historically, the use of surgical thalamotomy evolved to thalamic deep brain stimulation (DBS) mainly because of limitations in the treatment of bilateral brain lesions but also because of treatment possibilities introduced by neuromodulation. VIM DBS has been shown to reduce tremor by 50% to 90% at long-term follow-up (Benabid et al., 1996; Higuchi et al., 2015; Zhang et al., 2010). However, some patients are not ideal surgical candidates for open DBS procedures, and other approaches have been introduced, including stereotactic radiosurgery (SRS) (Campbell et al., 2015) and magnetic resonance–guided focused ultrasonography (MRgFUS) (Elias et al., 2016). These latter procedures are much more dependent on accurate imaging because intraoperative electrophysiologic recordings cannot be used to guide treatment.

Preoperative thalamic targeting methods have historically relied on indirect targeting mainly because individual thalamic nuclei are not well resolved with traditional neuroimaging methods. Standard target points can be identified in reference to universally applied coordinates to the anterior-posterior commissure line by using atlas-based methods or stereotaxy-based approaches (Abosch et al., 2010; Sudhyadhom et al., 2009). Importantly, these preoperative techniques do not fully account for variations in functional anatomy between patients. By using a preoperative thalamic segmentation scheme based on probabilistic diffusion tensor imaging, Middlebrooks et al. (Middlebrooks et al., 2018a) recently showed substantial inter- and intrasubject variability in structural connectivity compared with a fixed coordinate-based stereotactic target. Others have also shown some early success in applying these techniques to define single-subject connectivity profiles in small numbers of patients who underwent thalamic DBS, SRS, and MRgFUS (Kim et al., 2018; Pouratian et al., 2011; Tsolaki et al., 2018).

The described interindividual variations in thalamic functional anatomy may, in part, contribute to the reported variability in patient outcomes: improvement in tremor reportedly ranges from 18% to 88% (Wharen Jr. et al., 2017). In theory, improvements in preoperative targeting techniques may help increase the success rate of using thalamic DBS to treat tremor while reducing the incidence of adverse effects and also maximizing battery life. Therefore, the purpose of this study was to evaluate the potential of using structural connectivity–based segmentation (SCBS) of the thalamus as a preoperative targeting technique. We aimed to correlate location with improvement in tremor following VIM DBS. On the basis of the results of previous studies (Middlebrooks et al., 2018a; Pouratian et al., 2011) and the outcomes from rescue leads implanted in the ventralis oralis (VO) (Oyama et al., 2011; Yu et al., 2009), we hypothesized that increasing the volume of tissue activated (VTA) within the segment most connected to the supplementary motor area (SMA) and premotor cortex (PMC) would correlate with improvement in the clinical tremor score.

2. Materials and methods

2.1. Study patients

The study used a retrospective design and was approved by the University of Florida Institutional Review Board. An institutional database from the Center for Movement Disorders and Neurorestoration in Gainesville, Florida, of patients who received DBS was queried. Inclusion criteria were as follows: 1) the patient had a diagnosis of ET; 2) the patient received thalamic DBS for tremor; 3) the patient had no prior DBS lead placement; 4) a single lead was implanted during the first surgical procedure; 5) the Fahn-Tolosa-Marin Tremor Rating Scale (TRS) score (Stacy et al., 2007) was recorded immediately before the operation and at the 6-month follow-up; 6) the DBS programming settings were recorded; and 7) an appropriate imaging protocol was used that consisted of preoperative diffusion tensor imaging and postoperative high-resolution computed tomography for lead localization. Patients with dual leads that were placed at the initial surgery were excluded because the isolated effects of each lead could not be assessed. Patients who later underwent a second lead placement did not undergo evaluations of the second lead placement because the inclusion of such patients would have violated the statistical assumption of independent measurements.

A total of 40 such patients with ET who underwent DBS were identified. Demographic and disease information regarding age at DBS, sex, disease duration, and handedness were collected. DBS programming settings that corresponded to the greatest improvement in tremor without unintended adverse effects were also recorded. The TRS score was measured by a practitioner (who was blinded to the DBS parameters evaluated in this study due to the retrospective design) skilled in TRS measurement at a high-volume DBS and movement disorders clinic. TRS was measured at the pre-operative visit and at the 6-month follow-up; a greater TRS score representing worse symptoms. Two different outcomes were then calculated with regard to change in TRS score between the preoperative and 6-month follow-up time points. First, we assessed the raw change in the TRS score (preoperative score minus 6-month follow-up score). Second, the percentage change in the TRS score ([preoperative score minus 6-month follow-up score] divided by preoperative score) was measured. For each of these two separate change in TRS score outcomes, a greater change in the TRS score represented a greater improvement in symptoms from the preoperative to the 6-month follow-up visit.

2.2. Image acquisition

Imaging data were obtained from each patient's clinical preoperative magnetic resonance imaging (MRI) evaluation that was performed to plan DBS. For the purposes of this study, the imaging protocol included a postcontrast T1-weighted magnetization-prepared rapid gradient-echo (MP-RAGE) sequence and multidirectional diffusion-weighted imaging sequence. Each scan was obtained using a 3-T Siemens Verio system (Siemens AG, Healthcare Sector) with a 12-channel head coil.

The multidirectional diffusion-weighted imaging scan was acquired with the following parameters: isotropic resolution = $1.6 \times 1.6 \times 1.6$ mm with no gap; slices = 70; diffusion directions = 64; b value = 1000 s/mm^2; repetition time = 10,800 ms; echo time = 100 ms; phase partial Fourier = 5/8; generalized autocalibrating partially parallel acquisitions = 2; bandwidth = 1098 Hz/Px; and echo-planar imaging factor = 130. Six total volumes were also obtained with a b value = 0 s/mm^2. The total imaging time was 12:14 min.

MP-RAGE imaging was acquired in the axial plane after the administration of gadolinium-based intravenous contrast (0.1 mm/kg). The imaging parameters were as follows: in-plane resolution = 0.6×0.6 mm; slice thickness = 1.0 mm; repetition

time = 1720 ms; echo time = 3.29 ms; inversion time = 865 ms; flip angle = 9°; bandwidth = 170 Hz/Px; phase partial Fourier = 7/8; and generalized autocalibrating partially parallel acquisitions = 2. Image time was 5:16 min.

Postoperative computed tomography images were obtained using a Toshiba Aquilion scanner (Toshiba Medical Systems). Images were obtained with an in-plane resolution of 0.5×0.5 mm and 1-mm-thick slices. CT was obtained approximately one month after DBS implantation to minimize the possibility of brain shift or lead migration.

2.3. Surgical procedures for DBS

A DBS electrode (Model 3387; Medtronic Inc) was used to perform VIM thalamic DBS in each patient on the side contralateral to their most symptomatic upper extremity. We performed a high-resolution, volumetric brain MRI scan before the first procedure, and a Cosman-Roberts-Wells head ring was applied before performing a high-resolution, stereotactic head computed tomography scan on the day of surgery. The MRI and computed tomography scans were fused together using in-house software, and the target was chosen using postcontrast MP-RAGE and fast gray matter acquisition T1 inversion recovery MRI sequences that were paired with a deformable brain atlas to clarify the thalamic anatomy (Sudhyadhom et al., 2009). Microelectrode recordings were used to establish the locations of the anterior border of the ventralis caudalis and the sensorimotor hand area of the VIM.

Patients were observed overnight in the hospital before discharge home on postoperative day 1. An implantable pulse generator was implanted in a second, staged outpatient procedure while the patient was under general anesthesia at 1 month after discharge. After 6 months of stimulation, the follow-up TRS score was calculated for each patient. Tremor-suppressing medications were maintained at the preoperative dose for the study duration.

2.4. Imaging preprocessing

Diffusion data underwent standard preprocessing that consisted of realignment and eddy current correction using the Functional MRI of the Brain (FMRIB) Software Library (FSL) version 5.0.10. Using the "eddy" command, we utilized outlier detection with default parameters to assess for any slice in which the average intensity is at least four SDs less than expected as estimated by the Gaussian process prediction. Since head motion is a concern in patients with a tremor disorder, a stringent cutoff for head motion was used and any subjects with > 0.5% of all slices identified as an outlier were excluded from further analysis. This resulted in the exclusion of two subjects leaving a total of 40 subjects in the analysis. All preoperative MRI and postoperative CT images were co-registered using 2-stage linear registration that consisted of rigid and subsequent affine registration by using Advanced Normalization Tools (Avants et al., 2008). All volumes were then normalized to the MNI_ICBM_2009b_NLIN_ASYM atlas space using the symmetric image normalization and registration approach that is available by using Advanced Normalization Tools using the pre-operative MP-RAGE for generation of the transformation matrix (Avants et al., 2008; Fonov et al., 2011). Image registration was verified by a board certified Neuroradiologist via visual inspection using the "Check Results" feature of registration in the Lead-DBS software package (http://www.lead-dbs.org).

2.5. Regions of interest

Regions of interest were defined for each hemisphere separately in the Montreal Neurological Institute's template space and created using the FSLView "atlas" function. The cortical regions of interest for the primary motor cortex, primary sensory cortex, and SMA/PMC were generated from the Montreal Neurological Institute's Human Motor Area Template (HMAT) (Mayka et al., 2006). Masks for the prefrontal

cortex, occipital lobe, temporal lobe, and parietal lobe were generated by using the Harvard-Oxford cortical atlas. To account for variation between atlases, the HMAT regions of interest were subtracted from those generated by the Harvard-Oxford cortical atlas to ensure no overlap between ROIs. The thalamic regions of interest were generated by using the Harvard-Oxford subcortical atlas. All ROIs were manually verified for accuracy.

2.6. Diffusion data processing

The preprocessed diffusion data were used to estimate voxel-wise diffusion parameters by using Markov chain Monte Carlo sampling in FSL's "BEDPOSTX" function. FSL's "PROBTRACKX" function was used to perform probabilistic tractography and to calculate the probability of connecting each voxel in the left and right thalamic masks to each of the 7 previously defined cortical target masks. Tracking parameters included the following: total number of samples = 5000; curvature threshold = 0.2; step length = 0.5 mm; and maximum steps = 2000. All voxels within each thalamic mask were then classified by the 1 cortical target region with the greatest number of propagated paths by using FSL's "find_the_biggest" function. Each of the normalized 7 thalamic segments were averaged for all 40 patients to generate a group-level probability map for each segment. The probability map was thresholded to > 10% and binarized to generate a connectivity-based group atlas (Supplemental Fig. 2).

2.7. VTA modeling

The normalized postoperative computed tomography scan and Lead-DBS software package were used to accurately localize the final DBS electrode position (Horn and Kuhn, 2015). Next, VTA was estimated by using the finite element method and the patient's most effective programming settings, as implemented by Horn et al. (Horn et al., 2017) After VTA was estimated, the volume of overlap between the VTA and each of the 7 thalamic segments was calculated. Additionally, the volume of VTA overlap with the group-averaged SMA/PMC segment and primary motor segment was calculated to compare single-subject results with connectivity-based atlas results.

2.8. Statistical analysis

Continuous variables are summarized as median (range) values. Categorical variables are summarized as the number (percentage) of patients. Associations between the VTA of each thalamic segment (and also total VTA) and the change in the TRS score from the preoperative to 6-month follow-up visit (both raw change and percentage change) were evaluated using linear regression models. In addition to examining the unadjusted models, we also examined multivariable models that were adjusted for age at DBS, sex, disease duration, and side of DBS. Regression coefficients and 95% CI values were estimated and were interpreted as the change in the mean TRS score outcome that corresponded to a specified increase in VTA in the given thalamic segment. When fewer than 5 patients had a VTA > 0 mm³ for a given thalamic segment, associations with the change in TRS score outcomes was not assessed because of the lack of variability in the measurements. After excluding these thalamic segments, the association between change in TRS score (both raw change and percentage change) and VTA in 3 thalamic segments (prefrontal cortex, primary motor cortex, and SMA/PMC) and total VTA were evaluated. Spearman's correlation coefficient r was also estimated in order to further summarize the strength of correlation between VTA parameters and changes in TRS outcomes. After performing a Bonferroni correction for these 4 statistical tests, $P \le .0125$ was considered statistically significant, and all tests were 2-sided. Statistical analyses were performed using SAS (version 9.4; SAS Institute Inc) and R Statistical Software (version 3.2.3; R Foundation for Statistical Computing).

Table 1
Patient and DBS Characteristics and Outcomes.

Characteristics	Value (N = 40)
Patient characteristics	
Age at DBS, median (range), y	70 (39 to 84)
Men, No. (%)	24 (60)
Disease duration, median (range), y	19 (5 to 70)
Right handed, No. (%)	35 (87.5)
DBS characteristics	
Side of DBS, No. (%)	
Left	33 (82.5)
Right	7 (17.5)
Handedness/side of DBS	
Left/right or right/left	38 (95.0)
Left/left or right/right	2 (5)
Volume of tissue activated	
Occipital lobe	
> 0 mm^3, No. (%)	0 (0.0)
Median (range), mm^3	0 (0 to 0)
Posterior parietal lobe	
> 0 mm^3, No. (%)	0 (0.0)
Median (range), mm^3	0 (0 to 0)
Prefrontal cortex	
> 0 mm^3, No. (%)	27 (67.5)
Median (range), mm^3	20 (0 to 964)
Primary motor cortex	
> 0 mm^3, No. (%)	22 (55.0)
Median (range), mm^3	10 (0 to 552)
Primary sensory cortex	
> 0 mm^3, No. (%)	2 (5.0)
Median (range) mm^3	0 (0 to 3)
Supplementary motor area/premotor cortex	
> 0 mm^3, No. (%)	40 (100.0)
Median (range), mm^3	343 (2 to 1065)
Temporal lobe	
> 0 mm^3, No. (%)	0 (0.0)
Median (range), mm^3	0 (0 to 0)
Total volume of tissue activated	
Median (range), mm^3	1007 (294 to 2315)
Outcomes, median (range)	
Preoperative TRS	46 (21 to 74)
6-month follow-up TRS	24 (4 to 48)
Raw change in TRS	21 (−7 to 50)
Percentage change in TRS	41 (−30 to 90)

Abbreviations: DBS, deep brain stimulation; TRS, Tremor Rating Scale.

3. Results

The patient and DBS characteristics and the outcomes of the 40 patients are summarized in Table 1. The median (range) age at DBS was 70 (39–84) years, and 24 patients (60%) were men. The median (range) disease duration was 19 (5–70) years. Most patients (95.0%) underwent DBS on the opposite side of their dominant hand used for writing and eating. The median (range) preoperative TRS score was 46 (21–74), and the median (range) TRS score at the 6-month follow-up was 24 (4–48). This difference corresponded to a median (range) raw improvement in TRS of 21 points (7-point decrease to 50-point increase), and a median (range) percentage improvement in TRS of 41% (30% worsening to 90% improvement)

The thalamic segmentation results are summarized in Fig. 1 and mirror the segmentation patterns reported in prior studies (Middlebrooks et al., 2018a; Behrens et al., 2003). Of the 7 thalamic segments assessed, only 3 segments (prefrontal cortex, primary motor cortex, and SMA/PMC) had at least some VTA overlap in > 5 patients (Table 1); these segments and total VTA were examined for associations with the raw change in the TRS score (Table 2) and percentage change in TRS score (Supplemental Table 1). A significant association between higher VTA in the SMA/PMC segment and greater raw change in TRS score (i.e., greater improvement in symptoms) was noted in the unadjusted analysis (P = .001) and in the analysis adjusted for age at DBS, sex, disease duration, and side of DBS (P = .001) (Fig. 2). Specifically,

in the adjusted analysis, for every 50 mm^3 increase in VTA in the SMA/PMC segment, the mean improvement in the TRS score was 1.76 points (Table 2). This finding was consistent in analysis evaluating percentage change in TRS score; a higher VTA in the SMA/PMC segment was associated with a significantly greater percentage change in TRS score in both unadjusted analysis (P = .004) and adjusted analysis (P = .011) (Supplemental Table 1, Supplemental Fig. 1).

No significant associations between raw change in TRS score and VTA in the prefrontal cortex or primary motor cortex segments or total VTA were noted in either unadjusted or adjusted analysis (all $P \geq$ .064) (Table 2 and Fig. 2). Similarly, when examining percentage change in TRS, no significant associations with VTA in the prefrontal cortex or primary motor cortex segments or total VTA were observed (all $P \geq$ .13) (Supplemental Table 1, Supplemental Fig. 1). Exemplary subjects are shown in Fig. 3 and Supplemental Fig. 3. Neither the SMA/PMC segment (P = .44 for absolute change; P = .74 for percentage change) nor the primary motor segment (P = .8 for absolute change; P = .4 for percentage change) showed a significant correlation with TRS reduction in the group-averaged connectivity-based atlas.

4. Discussion

Our results suggest that SCBS of the thalamus is an independent predictor of tremor improvement after thalamic DBS. Specifically, we found a significant correlation between greater VTA in the segment most connected to the SMA/PMC (presumably the VO nucleus) and improvement in TRS score as measured by both raw change and percentage change. No significant correlation was found between VTA in the segment most connected to the primary motor cortex (presumably the VIM) and change in TRS score. These findings indicate that this method of preoperative thalamic segmentation may be a valuable supplement to current targeting methods for thalamic DBS and could be used to maximize tremor control. Lastly, utilizing a connectivity-based atlas generated from the same patient group failed to predict change in TRS score as well as the single-subject measures, highlighting the inferiority of of atlas-based measures.

Successful DBS requires accurate preoperative targeting. Widely used indirect thalamic targeting methods rely on atlas- or coordinate-based methods that do not fully account for variations in functional anatomy between patients. Structural connectivity profiles that use fixed coordinate-based targets in the thalamus are widely variable (Middlebrooks et al., 2018a). This issue may, in part, contribute to the variability reported in treatment outcomes (Wharen Jr. et al., 2017). Although the final electrode position is typically modified using microelectrode recordings, intraoperative macrostimulation, or both, these techniques introduce risk and burden. With each microelectrode recording pass or lead repositioning, the risk of hemorrhage or stroke may increase and the microlesion effect may further limit mapping and complicate intraoperative decision-making (Tonge et al., 2015; Maiti et al., 2016). Improvements in preoperative targeting would likely improve outcomes and reduce complications and stimulation-induced adverse effects. Additionally, noninvasive techniques, such as SRS and MRgFUS, may benefit from improved preoperative targeting because invasive electrophysiologic data cannot be used with these techniques. Finally, lead technologies, such as directional leads, and asleep DBS would also benefit from more accurate delineations of the ideal VTA (Chen et al., 2016).

The use of structural connectivity as a marker for DBS targeting and outcomes has been previously explored. Horn et al. (Horn et al., 2017) recently reported that structural connectivity in the subthalamic nucleus is an independent predictor of outcomes in patients with Parkinson disease who receive DBS. Middlebrooks et al. (Middlebrooks et al., 2018b) have also shown the potential of structural connectivity within the globus pallidus internus as an independent biomarker for DBS outcomes in Parkinson disease. Previous small clinical studies assessed the structural connectivity profiles in the thalamus used to guide
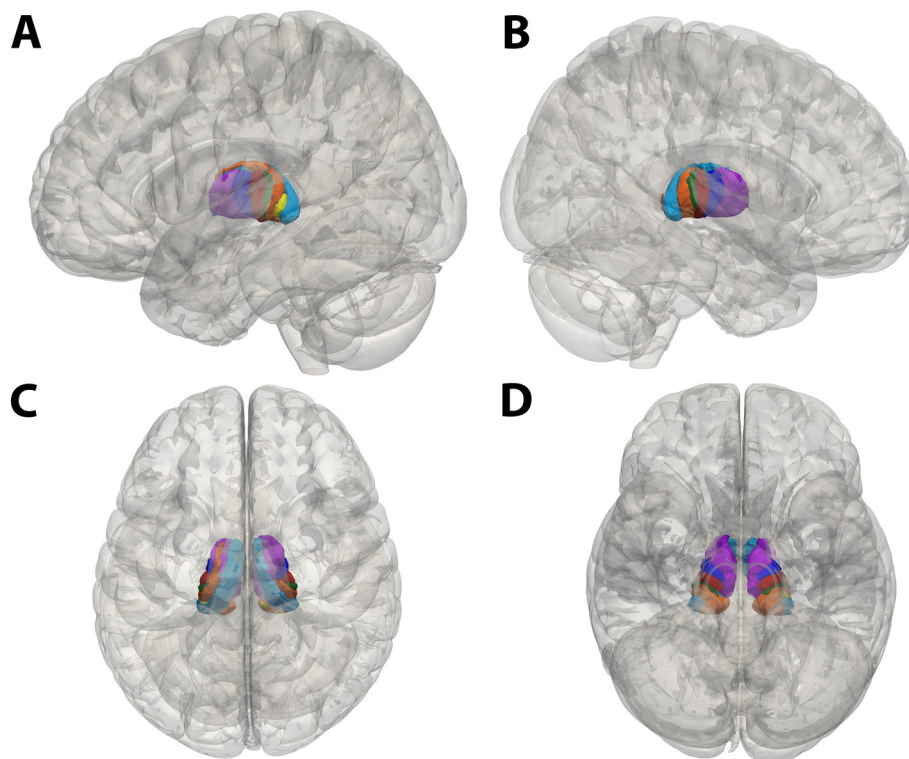
Fig. 1. Mean Group Thalamic Segmentation Results of 40 Patients. A, Left sagittal view showing the thalamic region most connected to the primary motor cortex (red), primary sensory cortex (green), supplementary motor area and premotor cortex (blue), occipital lobe (yellow), parietal lobe (orange), prefrontal cortex (purple), and temporal lobe (light blue). B, Right sagittal view showing the same regions. C, Superior view. D, Inferior view.

Table 2
Associations Between VTA and Raw Change in TRS Score for the 40 Patients with Essential Tremor.

Brain Segment (Increase in VTA)	Unadjusted Analysis[a]		Adjusted Analysis[a,b]	
	Regression Coefficient (95% CI)	P Value	Regression Coefficient (95% CI)	P Value
Prefrontal cortex (50 mm³)	−0.89 (−1.84 to 0.06)	0.064	−0.57 (−1.72 to 0.58)	0.32
Primary motor cortex (50 mm³)	1.93 (−0.18 to 4.04)	0.072	1.48 (−0.76 to 3.71)	0.19
Supplementary motor area/premotor cortex (50 mm³)	1.58 (0.75 to 2.41)	0.001	1.76 (0.76 to 2.76)	0.001
Total VTA (100 mm³)	0.12 (−1.19 to 1.42)	0.86	0.09 (−1.20 to 1.38)	0.89

Abbreviations: DBS, deep brain stimulation; TRS, Tremor Rating Scale; VTA, volume of tissue activated.

[a] Regression coefficients, 95% CIs, and P values were determined using linear regression models. The regression coefficient indicates the change in the mean raw change in TRS score (preoperative score minus the 6-month follow-up score) that corresponds to the increase in VTA shown in parentheses for each brain segment.

[b] Adjusted for age at deep brain stimulation, sex, disease duration, and side of DBS.

DBS, MRgFUS, and SRS procedures (Kim et al., 2018; Pouratian et al., 2011; Tsolaki et al., 2018). The correlation between SCBS and brain segments in patients who received DBS was first reported by Pouratian et al. (Pouratian et al., 2011); they found that the optimal DBS contact was closer to the segment most connected to the PMC than the primary motor cortex in a series of 6 patients with ET. Importantly, this novel pilot study had some notable limitations. The optimal DBS contact used was localized, but no VTA was determined from the stimulation parameters that were used to quantitatively assess the overlap between the thalamic segment and activated tissue. In addition, patients with bilateral leads were assessed, which may have limited the ability to discern the therapeutic effect of each DBS lead (Sandoe et al., 2018). Nevertheless, the insights provided by this pilot study have been applied to noninvasive techniques, including a case report of SRS thalamotomy and a report of series of 12 patients who underwent MRgFUS thalamotomy. These studies collectively support the finding of improved outcomes when using the thalamic region most connected to the PMC (Kim et al., 2018; Pouratian et al., 2011).

Importantly, other potential connectivity targets have been proposed for ET DBS, most notably the dentato-rubro-thalamic tract (Coenen et al., 2014; Coenen et al., 2011; Coenen et al., 2016; Coenen et al., 2017). Akram et al. (Akram et al., 2018) recently reported a comparison of probabilistic tractography–based thalamic segmentation with probabilistic fiber tracking of the dentato-rubro-thalamic tract in a series of patients with Parkinson disease and ET who underwent DBS. Their study reported that patients with a greater improvement in tremor score had more VTA overlap with the dentato-rubro-thalamic tract (thereby closely mirroring the probabilistic tractography–based primary motor cortex segment) rather than the thalamic SMA/PMC segment (Akram et al., 2018). The authors attributed this discrepancy in their findings compared with the findings of Pouratian et al. (Pouratian et al., 2011) to the poor angular resolution, spatial resolution, and angular contrast used in Pouratian et al.'s study (Akram et al., 2018). Despite these findings, we found similar results as reported by Pouratian et al. (Pouratian et al., 2011) in our protocol that utilized higher angular resolution and higher spatial resolution than the original studies of Pouratian et al. (Pouratian et al., 2011) The contradiction between our current study and Akram et al.'s study (Akram et al., 2018) could be related to the small number of patients enrolled in their study (40 vs 9 patients, respectively), thereby preventing statistical correlation, or due to the lack of significant stimulation within the SMA/PMC segment. Alternatively, the use of group mean values to describe thalamic segmentation in Akram et al.'s study (Akram et al., 2018) limits determination of the effects of DBS in each patient relative to VTA overlap in each segment, particularly given the known inter- and intrapatient variations (Middlebrooks et al., 2018a). Additionally, Nowacki et al. were unable to reproduce the correlation between dentato-rubro-thalamic proximity and tremor reduction (Nowacki et al., 2018).
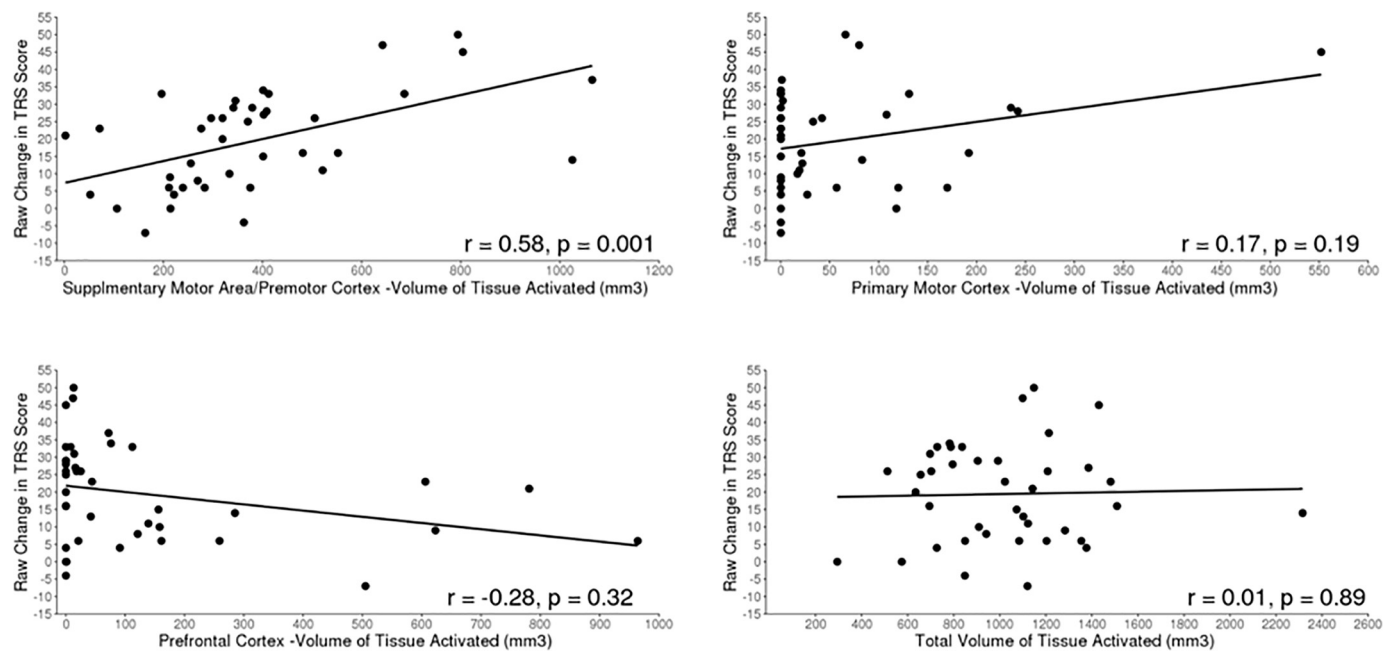
Fig. 2. Associations Between Raw Change in TRS Score and Volume of Tissue Activated in Different Brain Segments. A, Association between raw change in the TRS score from the preoperative visit to the 6-month follow-up (preoperative score minus 6-month follow-up score) and the volume of tissue activated in the SMA/PMC segment. B, Association between raw change in the TRS score and the volume of tissue activated in the primary motor cortex. C, Association between raw change in the TRS score and the volume of tissue activated in the prefrontal cortex. D, Association between raw change in the TRS score and the total volume of tissue activated. The regression line is shown with a solid line in all graphs. Spearman's correlation coefficient *r* is displayed in each graph along with the *p*-value from the multivariable linear regression analysis. PMC indicates premotor cortex; SMA, supplementary motor area; TRS, Tremor Rating Scale.
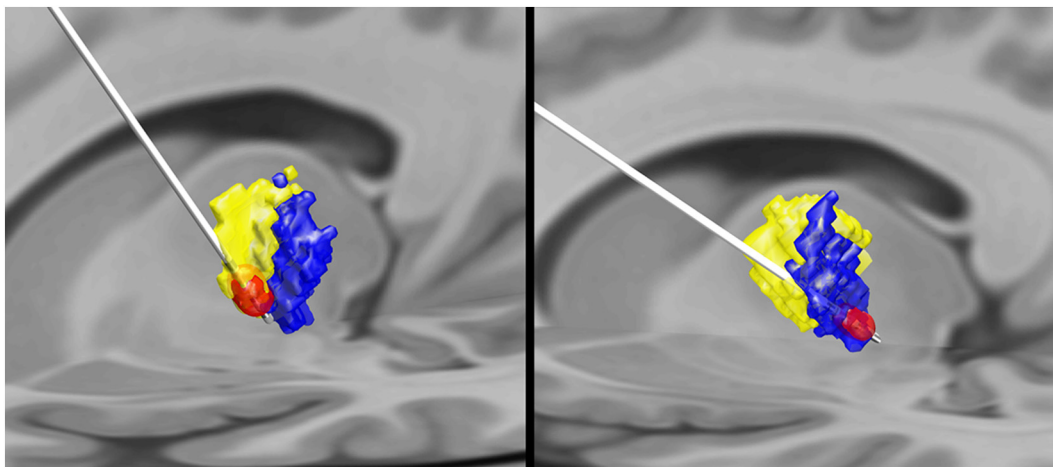

Fig. 3. Structural-connectivity based segmentation of two exemplary patients. The first patient (left) had a decrease in tremor rating score (TRS) from 63 to 16 (75% decrease) and shows greater overlap of the volume of tissue activated (red) with the region most connected with the supplementary motor area/premotor cortex (yellow). The second patient (right) shows greater overlap of the volume of tissue activated with the region most connected to the primary motor cortex (blue) and only had a decrease in TRS from 34 to 25 (26% decrease).

Because the thresholds for angular resolution, spatial resolution, and angular contrast needed to accurately assess the response to DBS have yet to be determined, attributing differences in outcomes to such imaging parameters is speculative, at this time. Future studies will be needed to further elucidate the basis of discrepancies in these collective studies.

In our current study of 40 patients who underwent VIM DBS for tremor, we showed the value of using SCBS to predict the degree of improvement in TRS score. By modeling VTA in each patient and by analyzing the volume of VTA overlap with each thalamic segment, we demonstrated that the VTA within the segment most connected to the SMA/PMC was correlated with tremor reduction as measured by the change in the TRS score. Our study design included only patients with

unilateral lead placement in order to avoid potential confounders related to the effects of DBS on ipsilateral tremor and to avoid violating the statistical assumption of independent measurements in patients with bilateral leads.

The mechanistic underpinnings of tremor control by VIM DBS remain debatable. While VIM has traditionally been considered the intended target, other DBS targets have been suggested such as the subthalamic nucleus (Benabid et al., 2009), prelemniscal radiations (Velasco et al., 2001), VO thalamic nucleus (Foote et al., 2006), caudal zona incerta (Plaha et al., 2008), and dentato-rubro-thalamic tract (Coenen et al., 2014; Coenen et al., 2017). Because no specific target or targeting mechanism has been shown to be entirely predictive of outcomes, the underlying pathophysiology and treatment effects are likely

multifactorial. However, our finding that the ideal VTA overlaps with the SMA/PMC segment (presumably the VO nucleus) was corroborated by electrophysiologic and clinical studies that showed effective tremor reduction with VO stimulation (Foote and Okun, 2005; Foote et al., 2006; Ramirez-Zamora and Okun, 2016; Yamamoto et al., 2004). The effect of VO stimulation has also been clinically shown with improvement in tremor control in patients whose VIM DBS initially failed. In these cases, a VO rescue lead was placed anterior to the previously placed VIM lead (Oyama et al., 2011; Servello et al., 2009). Other groups have proposed that stimulation of the pallidal-receiving neurons in the VO region of the thalamus may be another therapeutic target for tremor control (Mehanna et al., 2014; Yu et al., 2009; Foote et al., 2006).

Several limitations of our study are noteworthy. First, because of the relatively small sample size, there was limited power to detect associations between VTA and changes in the TRS scores. Although we were able to demonstrate a significant association between VTA in the SMA/PMC region and change in TRS score despite this lack of power, the possibility of a type II error (ie, a false-negative finding) is important when considering the other findings. Second, a greater number of patients had a preferential stimulation in the SMA/PMC segment relative to the M1 segment. While this is potentially a bias introduced by the use of intra-operative recordings resulting in repositioning of the target in attempt to achieve maximum therapeutic response, this is speculative given the retrospective nature of the study. Similar positional stimulation bias in other studies limits comparability of treatment response with each target and future studies are needed to fully elucidate the difference in effect of both targets (Akram et al., 2018). Third, spatial precision in functional neurosurgery is critically important; however, the ideal spatial resolution for accurate targeting with diffusion tensor imaging is currently unknown. Likewise, the accuracy of segmentation is potentially limited by the angular resolution of diffusion tensor imaging, and the number of ideal diffusion directions remains unknown. Our study, in contradistinction from several prior studies, used higher angular and spatial resolution yet found similar results (Kim et al., 2018; Pouratian et al., 2011; Tsolaki et al., 2018; Coenen et al., 2017). Interestingly, the only similar study using even higher spatial and angular resolution reported contradictory results, which may have been related to the small sample size and use of group mean thalamic segmentation values (Akram et al., 2018). Unfortunately, because multiple protocols were not tested to compare these methods, it remains unknown if these factors will alter potential target points and stimulation volumes. Lastly, the geometric distortion inherent to echo-planar imaging may affect spatial localization after rigid image registration, and these changes could not be completely corrected in this retrospective data set. Our future acquisition methods will implement more accurate methods to estimate the susceptibility-induced off-resonance field for distortion correction and could be used to ascertain the potential effects on spatial localization of thalamic segments. Despite these limitations, the predictability of the proposed model and associated tremor outcomes is intriguing and warrants continued investigation.

5. Conclusions

The results of this study suggest that a larger VTA in the SMA/PMC thalamic segment during DBS is associated with a significant improvement in TRS scores in patients with ET. No associations between change in TRS score and VTA in the prefrontal cortex or primary motor cortex segments or total VTA were noted. Although prospective studies are needed to validate the added benefit of SCBS compared with traditional indirect targeting methods alone, our findings support the potential role of thalamic SCBS as an independent preoperative predictor of tremor improvement in patients who undergo VIM DBS.

Appendix A. Supplementary data

Supplementary data to this article can be found online at https://doi.org/10.1016/j.nicl.2018.10.009.

References

Abosch, A., Yacoub, E., Ugurbil, K., Harel, N., 2010. An assessment of current brain targets for deep brain stimulation surgery with susceptibility-weighted imaging at 7 tesla. Neurosurgery 67 (6), 1745–1756 (discussion 1756).

Akram, H., Dayal, V., Mahlknecht, P., et al., 2018. Connectivity derived thalamic segmentation in deep brain stimulation for tremor. Neuroimage Clin. 18, 130–142.

Avants, B.B., Epstein, C.L., Grossman, M., Gee, J.C., 2008. Symmetric diffeomorphic image registration with cross-correlation: evaluating automated labeling of elderly and neurodegenerative brain. Med. Image Anal. 12 (1), 26–41.

Behrens, T.E., Johansen-Berg, H., Woolrich, M.W., et al., 2003. Non-invasive mapping of connections between human thalamus and cortex using diffusion imaging. Nat. Neurosci. 6 (7), 750–757.

Benabid, A.L., Pollak, P., Gao, D., et al., 1996. Chronic electrical stimulation of the ventralis intermedius nucleus of the thalamus as a treatment of movement disorders. J. Neurosurg. 84 (2), 203–214.

Benabid, A.L., Chabardes, S., Mitrofanis, J., Pollak, P., 2009. Deep brain stimulation of the subthalamic nucleus for the treatment of Parkinson's disease. Lancet Neurol. 8 (1), 67–81.

Campbell, A.M., Glover, J., Chiang, V.L., Gerrard, J., Yu, J.B., 2015. Gamma knife stereotactic radiosurgical thalamotomy for intractable tremor: a systematic review of the literature. Radiother. Oncol. 114 (3), 296–301.

Chen, T., Mirzadeh, Z., Chapple, K., Lambert, M., Dhall, R., Ponce, F.A., 2016. "Asleep" deep brain stimulation for essential tremor. J. Neurosurg. 124 (6), 1842–1849.

Coenen, V.A., Allert, N., Madler, B., 2011. A role of diffusion tensor imaging fiber tracking in deep brain stimulation surgery: DBS of the dentato-rubro-thalamic tract (drt) for the treatment of therapy-refractory tremor. Acta Neurochir. 153 (8), 1579–1585 (discussion 1585).

Coenen, V.A., Allert, N., Paus, S., Kronenburger, M., Urbach, H., Madler, B., 2014. Modulation of the cerebello-thalamo-cortical network in thalamic deep brain stimulation for tremor: a diffusion tensor imaging study. Neurosurgery 75 (6), 657–669 (discussion 669–670).

Coenen, V.A., Rijntjes, M., Prokop, T., et al., 2016. One-pass deep brain stimulation of dentato-rubro-thalamic tract and subthalamic nucleus for tremor-dominant or equivalent type Parkinson's disease. Acta Neurochir. 158 (4), 773–781.

Coenen, V.A., Varkuti, B., Parpaley, Y., et al., 2017. Postoperative neuroimaging analysis of DRT deep brain stimulation revision surgery for complicated essential tremor. Acta Neurochir. 159 (5), 779–787.

Dogu, O., Sevim, S., Camdeviren, H., et al., 2003. Prevalence of essential tremor: door-to-door neurologic exams in Mersin Province, Turkey. Neurology 61 (12), 1804–1806.

Elias, W.J., Lipsman, N., Ondo, W.G., et al., 2016. A randomized trial of focused ultrasound thalamotomy for essential tremor. N. Engl. J. Med. 375 (8), 730–739.

Fonov, V., Evans, A.C., Botteron, K., et al., 2011. Unbiased average age-appropriate atlases for pediatric studies. NeuroImage 54 (1), 313–327.

Foote, K.D., Okun, M.S., 2005. Ventralis intermedius plus ventralis oralis anterior and posterior deep brain stimulation for posttraumatic Holmes tremor: two leads may be better than one: technical note. Neurosurgery 56 (2 Suppl), E445 discussion E445.

Foote, K.D., Seignourel, P., Fernandez, H.H., et al., 2006. Dual electrode thalamic deep brain stimulation for the treatment of posttraumatic and multiple sclerosis tremor. Neurosurgery 58 (4 Suppl 2) ONS-280-285; discussion ONS-285-286.

Higuchi, M.A., Topiol, D.D., Ahmed, B., et al., 2015. Impact of an interdisciplinary deep brain stimulation screening model on post-surgical complications in essential tremor patients. PLoS One 10 (12), e0145623.

Horn, A., Kuhn, A.A., 2015. Lead-DBS: a toolbox for deep brain stimulation electrode localizations and visualizations. NeuroImage 107, 127–135.

Horn, A., Reich, M., Vorwerk, J., et al., 2017. Connectivity predicts deep brain stimulation outcome in Parkinson disease. Ann. Neurol. 82 (1), 67–78.

Kim, W., Sharim, J., Tenn, S., et al., 2018. Diffusion tractography imaging-guided frameless linear accelerator stereotactic radiosurgical thalamotomy for tremor: case report. J. Neurosurg. 128 (1), 215–221.

Louis, E.D., 2001. Clinical practice. Essential tremor. N. Engl. J. Med. 345 (12), 887–891.

Louis, E.D., Ottman, R., 2014. How many people in the USA have essential tremor? Deriving a population estimate based on epidemiological data. Tremor Other. Hyperkinet. Mov. 4, 259.

Maiti, T.K., Konar, S., Bir, S., Kalakoti, P., Nanda, A., 2016. Intra-operative micro-electrode recording in functional neurosurgery: past, present, future. J. Clin. Neurosci. 32, 166–172.

Mayka, M.A., Corcos, D.M., Leurgans, S.E., Vaillancourt, D.E., 2006. Three-dimensional locations and boundaries of motor and premotor cortices as defined by functional brain imaging: a meta-analysis. NeuroImage 31 (4), 1453–1474.

Mehanna, R., Machado, A.G., Oravivattanakul, S., Genc, G., Cooper, S.E., 2014. Comparing two deep brain stimulation leads to one in refractory tremor. Cerebellum (London, England) 13 (4), 425–432.

Middlebrooks, E.H., Holanda, V.M., Tuna, I.S., et al., 2018a. A method for pre-operative single-subject thalamic segmentation based on probabilistic tractography for essential tremor deep brain stimulation. Neuroradiology 60 (3), 303–309.

Middlebrooks, E., Tuna, I., Grewal, S., et al., 2018 Junb. Segmentation of the globus pallidus internus using probabilistic diffusion tractography for deep brain stimulation targeting in Parkinson disease. AJNR Am. J. Neuroradiol. 39 (6), 1127–1134. https://doi.org/10.3174/ajnr.A5641. Epub 2018 Apr 26.

Nowacki, A., Schlaier, J., Debove, I., Pollo, C., 2018. Validation of diffusion tensor imaging tractography to visualize the dentatorubrothalamic tract for surgical planning. J. Neurosurg. 1–10.

Oyama, G., Foote, K.D., Hwynn, N., et al., 2011. Rescue leads: a salvage technique for selected patients with a suboptimal response to standard DBS therapy. Parkinsonism Relat. Disord. 17 (6), 451–455.

Plaha, P., Khan, S., Gill, S.S., 2008. Bilateral stimulation of the caudal zona incerta nucleus for tremor control. J. Neurol. Neurosurg. Psychiatry 79 (5), 504–513.

Pouratian, N., Zheng, Z., Bari, A.A., Behnke, E., Elias, W.J., Desalles, A.A., 2011. Multi-institutional evaluation of deep brain stimulation targeting using probabilistic connectivity-based thalamic segmentation. J. Neurosurg. 115 (5), 995–1004.

Ramirez-Zamora, A., Okun, M.S., 2016. Deep brain stimulation for the treatment of uncommon tremor syndromes. Expert. Rev. Neurother. 16 (8), 983–997.

Sandoe, C., Krishna, V., Basha, D., et al., 2018 May - Jun. Predictors of deep brain stimulation outcome in tremor patients. Brain Stimul. 11 (3), 592–599.

Servello, D., Sassi, M., Brambilla, A., et al., 2009. De novo and rescue DBS leads for refractory Tourette syndrome patients with severe comorbid OCD: a multiple case report. J. Neurol. 256 (9), 1533–1539.

Stacy, M.A., Elble, R.J., Ondo, W.G., Wu, S.C., Hulihan, J., Group TRSs, 2007. Assessment of interrater and intrarater reliability of the Fahn-Tolosa-Marin Tremor Rating Scale in essential tremor. Mov. Disord. 22 (6), 833–838.

Sudhyadhom, A., Haq, I.U., Foote, K.D., Okun, M.S., Bova, F.J., 2009. A high resolution and high contrast MRI for differentiation of subcortical structures for DBS targeting: the Fast Gray Matter Acquisition T1 Inversion Recovery (FGATIR). NeuroImage 47 (Suppl. 2), T44–T52.

Tonge, M., Ackermans, L., Kocabicak, E., et al., 2015. A detailed analysis of intracerebral hemorrhages in DBS surgeries. Clin. Neurol. Neurosurg. 139, 183–187.

Tsolaki, E., Downes, A., Speier, W., Elias, W.J., Pouratian, N., 2018. The potential value of probabilistic tractography-based for MR-guided focused ultrasound thalamotomy for essential tremor. NeuroImage Clin. 17, 1019–1027.

Velasco, F., Jimenez, F., Perez, M.L., et al., 2001. Electrical stimulation of the pre-lemniscal radiation in the treatment of Parkinson's disease: an old target revised with new techniques. Neurosurgery 49 (2), 293–306 (discussion 306-298).

Wharen Jr., R.E., Okun, M.S., Guthrie, B.L., et al., 2017. Thalamic DBS with a constant-current device in essential tremor: a controlled clinical trial. Parkinsonism Relat. Disord. 40, 18–26.

Yamamoto, T., Katayama, Y., Kano, T., Kobayashi, K., Oshima, H., Fukaya, C., 2004. Deep brain stimulation for the treatment of parkinsonian, essential, and poststroke tremor: a suitable stimulation method and changes in effective stimulation intensity. J. Neurosurg. 101 (2), 201–209.

Yu, H., Hedera, P., Fang, J., Davis, T.L., Konrad, P.E., 2009. Confined stimulation using dual thalamic deep brain stimulation leads rescues refractory essential tremor: report of three cases. Stereotact. Funct. Neurosurg. 87 (5), 309–313.

Zhang, K., Bhatia, S., Oh, M.Y., Cohen, D., Angle, C., Whiting, D., 2010. Long-term results of thalamic deep brain stimulation for essential tremor. J. Neurosurg. 112 (6), 1271–1276.